Journal of Enzyme Inhibition, Vol. 16, pp. 391–399
Reprints available directly from the publisher
Photocopying permitted by license only

Progress Curves Analysis as an Alternative for Exploration of Activation-inhibition Phenomena in Cholinesterases

MARKO GOLIČNIK

Institute of Biochemistry, Medical Faculty, University of Ljubljana, Vrazov trg 2, 1000 Ljubljana, Slovenia

(Received 1 May 2001)

The kinetic behaviour of insect acetylcholinesterases deviates from the Michaelis–Menten pattern. These deviations are known as activation or inhibition at various substrate concentrations and can be more or less observable depending on mutations around the active site of the enzyme. Most kinetic studies on these enzymes still rely on initial rate measurements. It is demonstrated here that according to this method one of the deviations can be overlooked. We attempt to point out that in such cases a detailed step-by-step progress curves analysis is successful. The study is focused on two different methods of analysing progress curves: (i) the first one is based on an integrated initial rate equation which can sufficiently fit truncated progress curves under corresponding conditions; and (ii) the other one precludes the algebraic formulae, but uses numerical integration for searching a non analytical solution of ordinary differential equations describing a kinetic model. All methods are tested on three different acetylcholinesterase mutants from *Drosophila melanogaster*. The results indicate that kinetic parameters for the E107K mutant with highly expressive activation and inhibition can be well evaluated applying any analysis method. It is quite different for E107W and E107Y mutants where latent activation is present, but discovered only using one or the other progress curves analysis methods.

Keywords: Enzyme kinetics; Progress curves; Rate equations; Numerical integration; Cholinesterases

Abbreviations: AChE: acetylcholinesterase; ATCh: acetylthiocholine; DTNB: 5,5′-dithio-bis-nitrobenzoic acid

INTRODUCTION

The development of site-directed mutagenesis has offered a new approach in enzyme research. This technique enables a systematic study of individual amino acid residue functions around the catalytic site. A great number of mutants can be obtained and their characterisation can lead to time-consuming work. In order to avoid wasting time and material it is necessary to apply such experimental and data analysis methods which could reduce the required work to a minimum. Moreover, it should be emphasized that in any case procedures used must not disturb the true events going on during the experiment.

*Tel.: +386-1-5437651. Fax: +386-1-5437641. E-mail: golicnik@ibmi.mf.uni-lj.si.

Kinetics is very useful in such investigations and plays an important role in enzymology. The results obtained with various methods and combined with crystallographic data provide novel information on the nature of enzyme catalysis. The usual way in which the reaction is monitored is by measuring the amount of reactant remaining or product formed at different times. The correctness of enzyme kinetic parameters determined from the time course of the reaction depends on the proposed model and the analysis of measured data. The entire procedure demands a certain degree of precision and criticism as shown in this paper.

Three different approaches to the analysis of progress curves obtained by the measuring of released thiocholine from acetylthiocholine in the cholinesterase catalysed reaction are represented in this work. The progress curves are treated by the following analyses: initial rate equation method; integrated rate equation method; and numerical integration method. We have chosen three various *Drosophila melanogaster* acetylcholinesterase mutants obtained by site-directed mutagenesis and with apparently different characteristics in their kinetic behaviour in this study. Our study was concentrated on the advantages and limitations of individual analysis methods and the aim was to justify the more complex progress curves analysis application.

EXPERIMENTAL

Theory

Insects possess a single acetylcholinesterase which shows the biphasic activation-inhibition kinetics[1] also seen with human BChE.[2] The reaction mechanism responsible for both phenomena is still not clear. Many models have been proposed to explain diversity from Michaelis–Menten kinetics[3,4] but none has been able to describe activation and inhibition simultaneously. Recently, a six parameter model was introduced by Stojan *et al.*[5] (Scheme 1) and it is operative for all cholinesterases in the absence as well as in the presence of various reversible and irreversible inhibitors.[2,6,7]

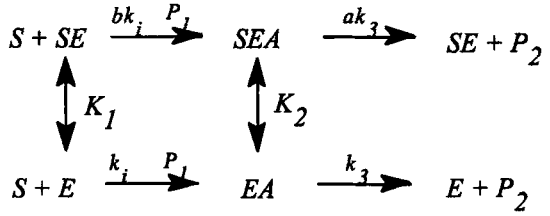

SCHEME 1

In this scheme, E is the free enzyme, EA is the acylated enzyme, and SE and SEA represent the complexes with the substrate molecule bound at the modulation site. Products P_1 and P_2 are thiocholine and acetate, respectively.

The model referred to in Scheme 1 assumes that apparent activation results from the binding of a substrate molecule to a modulation site of free enzyme affecting the acylation (factor b) while substrate bound to the acylated enzyme is responsible for decreased deacylation (factor a) and, therefore, leads to inhibition.

Initial Rate Equation

The initial rate equation for the model in Scheme 1 derived under the combined steady-state and equilibrium assumptions[8] can be written as:

$$v_0 = \frac{k_3[E_0][S_0]\left(1 + a\frac{[S_0]}{K_2}\right)}{[S_0]\left(1 + \frac{[S_0]}{K_2}\right) + \frac{k_3\left(1+a\frac{[S_0]}{K_2}\right)\left(1+\frac{[S_0]}{K_1}\right)}{k_i\left(1+b\frac{[S_0]}{K_1}\right)}} \quad (1)$$

$[E_0]$ and $[S_0]$ are total enzyme and starting substrate concentrations, respectively.

Integrated Rate Equation

Two different integrated rate equations can be derived from Eq. (1) for different experimental

conditions. At high substrate concentrations when depletion of substrate is negligible in comparison to the amount of recorded product (steady state assumptions) and the product concentration is a linear function of time, the following explicit function of $[P]_t$ can be used:

$$[P]_t = \frac{k_3[E_0][S_0]\left(1 + a\frac{[S_0]}{K_2}\right)}{[S_0]\left(1 + \frac{[S_0]}{K_2}\right) + \frac{k_3\left(1+a\frac{[s_0]}{K_2}\right)\left(1+\frac{[s_0]}{K_1}\right)}{k_i\left(1+b\frac{[s_0]}{K_1}\right)}} \cdot t \quad (2)$$

$[P]_t$ and t are time course of product concentration and time, respectively.

Equation (2) is useless when the mentioned conditions are not fulfilled and the substrate concentrations cannot be fixed during the measurement. This happens at substrate concentration low enough to avoid inhibition. In that case, the fraction in Eq. (1) can be reduced by an expression characterising substrate inhibition. The insertion of a time dependent measured product concentration into reduced Eq. (1) followed by integration leads to:

$$k_3[E_0]t = [P]_t - \frac{k_3}{k_i}\ln\left(1 - \frac{[P]_t}{[S_0]}\right) - \frac{k_3(1-b)}{k_i b}\ln\left(1 - \frac{b[P]_t}{(K_1 + b[S_0])}\right) \quad (3)$$

Fitting of this integrated rate equation necessarily involves repeated calculation of the expected value of $[P]_t$ for particular values of kinetic parameters, t and $[S_0]$. This is not a straightforward task, since Eq. (3) is an implicit function of $[P]_t$. The presence of both linear and logarithmic terms in $[P]_t$ precludes rearrangements of Eq. (3) into a form where $[P]_t$ is expressed as a function of the remaining quantities. Consequently, $[P]_t$ must be approximated by using an iterative procedure.

Numerical Integration Method

During the course of enzyme reactions in which a complete conversion of the reactants into the products occurs, the assumptions for the derivation of steady-state rate equations become violated. The integrated rate equation is not appropriate for the analysis of such complete progress curves. Non-linearity of ordinary differential equations does not enable the exact derivation of solutions for progress curves equations. Therefore, the analysis must be based on a numerical integration method. It was demonstrated that a semi-implicit midpoint rule extrapolation method,[9] designed for the numerical solutions of stiff systems of ordinary differential equations, can be very useful by analysing progress curves measured at similar conditions as those presented in our study.[10]

Experiments

Chemicals

Acetylthiocholine (ATCh) and 5,5′-dithio-bis-nitrobenzoic acid (DTNB, Ellman's reagent) were purchased from Sigma Chemical Co. (St. Louis, USA). All salts and buffers were of analytical grade. The experiments were carried out at 25°C in 25 mM sodium phosphate buffer and pH 7.

Source of Enzymes

Drosophila melanogaster AChE mutants (E107K, E107W and E107Y) were a gift from Dr Didier Fournier, Université Paul Sabatier, Toulouse, France. The enzymes were produced in baculovirus infected cells,[11] purified and stabilised with BSA.[12] Enzyme active sites titration was carried out using 7-(methylethoxyphosphinyloxy)-1-methylquinolinium iodide (MEPQ).

Kinetic Experiments

The hydrolysis of ATCh catalysed by all AChEs was recorded on a stopped-flow apparatus. Aliquots of two solutions, one containing only the selected enzyme and the other the substrate and Ellman's reagent were mixed together in the mixing chamber of the apparatus. The absorbance of the thiolate dianion of DTNB was monitored spectrophotometrically at 412 nm, according to Ellman *et al.*,[13] at concentrations of substrate from 5 μM to 50 mM and with 1 mM final concentration of reagent. At low substrate concentration, the reaction was followed to completion, while at higher concentrations only the initial portions were measured. In order to avoid possible product modulation, the measurement was stopped when 50 μM product was formed.

Data Analysis

The evaluation of corresponding kinetic parameters was carried out in three steps. (i) For the first estimation, a steady-state rate equation (Eq. (1)) was used. The equation was fitted to the initial rates obtained with data differentiation (tangents) at time zero of each progress curve. (ii) In the second step, the calculated parameters were inserted as initial estimates into integrated initial rate equations (Eqs. (2), (3)). The improved rearranged Eq. (3) proposed

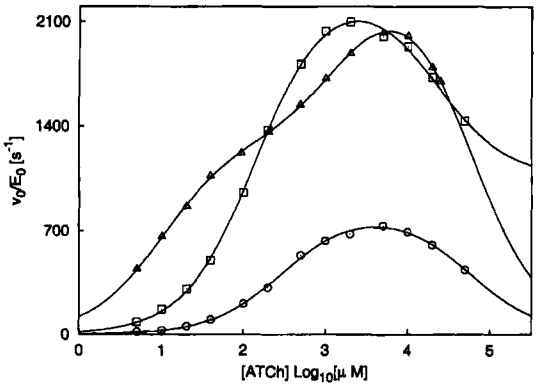

FIG. 1 *p*S curves for the hydrolysis of acetylthiocholine catalysed by various insect AChEs: (△), E107K mutant (0.60 nM); (□), E107W mutant (0.56 nM); and (○), E107Y mutant (2.43 nM).

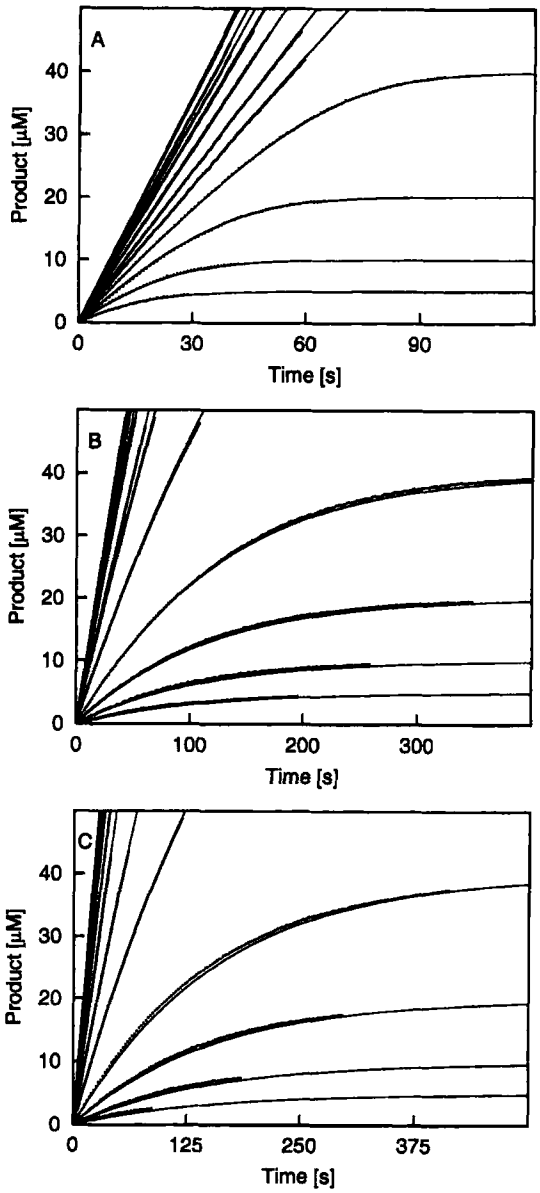

FIG. 2 Integrated initial rate equation fitted on truncated progress curves for the hydrolysis of acetylthiocholine by various *Drosophila melanogaster* AChEs: A, E107K; B, E107W; and C; E107Y. In panel A the complete integrated initial rate equation is applied, but not in panels B and C (see text). Only those parts of experimental progress curves where steady-state assumption is still valid (see text) are shown. Substrate concentrations are from 5 μM to 50 mM.

TABLE 1 Characteristics constants and calculated S.D. evaluated with different analysis methods for interactions of various insect cholinesterases with acetylthiocholine according to Scheme 1. (- Not considered in the model; D.P., determined previously; N.C., parameters do not converge.) Each set of progress curves contains approximately 1500 experimental data points

	E107K	E107W	E107Y
	A. Initial rate equation		
k_i ($M^{-1}s^{-1}$)	$1.24\times10^8 \pm 6\times10^6$	$1.65\times10^7 \pm 5\times10^5$	$2.74\times10^6 \pm 1\times10^4$
k_3 (s^{-1})	2466 ± 69	2349 ± 27	832 ± 12
K_1 (μM)	22 ± 2	–	–
K_2 (mM)	59 ± 6	21 ± 4	56 ± 4
a	0*	0.45 ± 0.03	0*
b	0.027 ± 0.004	–	–
	B. Integrated initial rate I		
k_i ($M^{-1}s^{-1}$)	$1.442\times10^8 \pm 4\times10^5$	$1.735\times10^7 \pm 2\times10^4$	$2.871\times10^6 \pm 3\times10^3$
k_3 (s^{-1})	2413 ± 2	2289 ± 2	827 ± 1
K_1 (μM)	18.48 ± 0.06	–	–
K_2 (mM)	64.2 ± 0.2	26.6 ± 0.3	58.1 ± 0.1
a	0*	0.428 ± 0.002	0*
b	0.02308 ± 0.00008	–	–
	C. Integrated initial rate II		
k_i ($M^{-1}s^{-1}$)	D.P.	$2.130\times10^7 \pm 2\times10^4$	N.C.
k_3 (s^{-1})	D.P.	2323 ± 2	N.C.
K_1 (μM)	D.P.	7.1 ± 0.7	N.C.
K_2 (mM)	D.P.	23.0 ± 0.2	N.C.
a	D.P.	0.443 ± 0.001	N.C.
b	D.P.	0.773 ± 0.008	N.C.
	D. Numerical integration		
k_i ($M^{-1}s^{-1}$)	$1.447\times10^8 \pm 4\times10^5$	$2.10\times10^7 \pm 2\times10^5$	$3.24\times10^6 \pm 4\times10^4$
k_3 (s^{-1})	2402 ± 2	2333 ± 1	833.2 ± 0.6
K_1 (μM)	18.45 ± 0.07	7.5 ± 0.6	14 ± 3
K_2 (mM)	65.2 ± 0.2	22.0 ± 0.2	56.8 ± 0.1
a	0*	0.447 ± 0.001	0*
b	0.0238 ± 0.0001	0.784 ± 0.006	0.864 ± 0.009

*Approaching zero.

by Duggleby[14] (see the Appendix) was fitted to the progress curves measured at low substrate concentrations (<0.5 mM) using the Newton–Raphson method. Taken into consideration were only those parts of progress curves where steady-state assumptions were still valid ([S]>1000[E_0]).[15] Equation (2) was used for fitting the non-curved progress curves data obtained at high substrate concentration. (iii) The new corrected kinetic and equilibrium constants were the starting-points for the last step. The differential equations for all species shown in Scheme 1 were derived as described previously[6,10] and fitted again to entire progress curves even those where plateaus were reached.

A non-linear regression computer program written by Stojan[10] was applied in all steps.

RESULTS

The results could be divided into four sections, in the order that the data analysis was performed. They are presented in Figs. 1–4. It should be noted that all four figures show the same data, but in different forms and fitted according to the various analysis methods.

Figure 1 displays data in the v_0/E_0 vs. pS form. The individual characteristics of enzymes can be shown in the most informative way from such pS curves. It can be seen that the substrate inhibition is present at high substrate concentrations in all mutants, while apparent substrate activation is obvious only in the E107K mutant. Therefore, Eq. (1) was fitted to initial rate data for the E107K mutant, but we used a reduced form without

algebraic terms responsible for apparent activation (expressions with K_1 and/or b) in the other two cases. All parameters determined in this way are shown in Table I, section A.

The kinetic constants presented in Table I under section A were put into Eqs. (2) and (3) and fitted to truncated progress curves. It should be borne in mind that the mathematical terms containing parameters b and K_1 were omitted in the case of mutants showing no apparent activation in the first step. The results are shown in Fig. 2 and the estimated constants in Table I, section B. Attention should be paid to two characteristics: (i) linear progress curves at high substrate concentration fit successfully in all tested AChEs; and (ii) theoretical progress curves describe initial portions of all progress curves very well including those at low substrate concentration, but they deviate early from experimental data for E107W and E107Y mutants (Fig. 2B, C). Obviously, substrate activation also had to be taken into consideration in the analysis of data obtained with the latter two mutants. So, the complete integrated initial rate Eqs. (2) and (3) were fitted to the data in Fig. 2B and C. Unfortunately, the fitting was successful only in the case of the E107W mutant as displayed in Fig. 3.

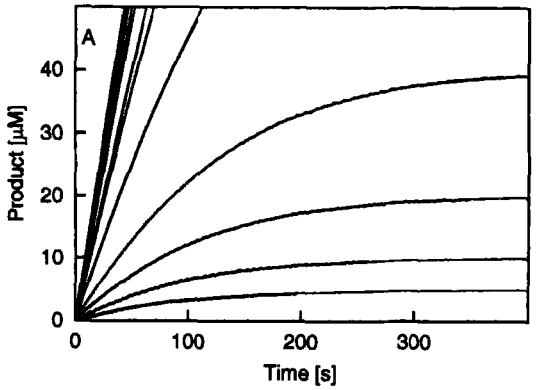

FIG. 3 The complete integrated initial rate equation fitted on the same progress curves given in Fig. 2 panel B (E107W mutant).

Finally, it can be seen from Fig. 4 that the numerically solved system of differential equations using a six parameter model (Scheme 1) fits remarkably well to all three sets of complete progress curves. Latent apparent substrate activation referring to the E107Y mutant

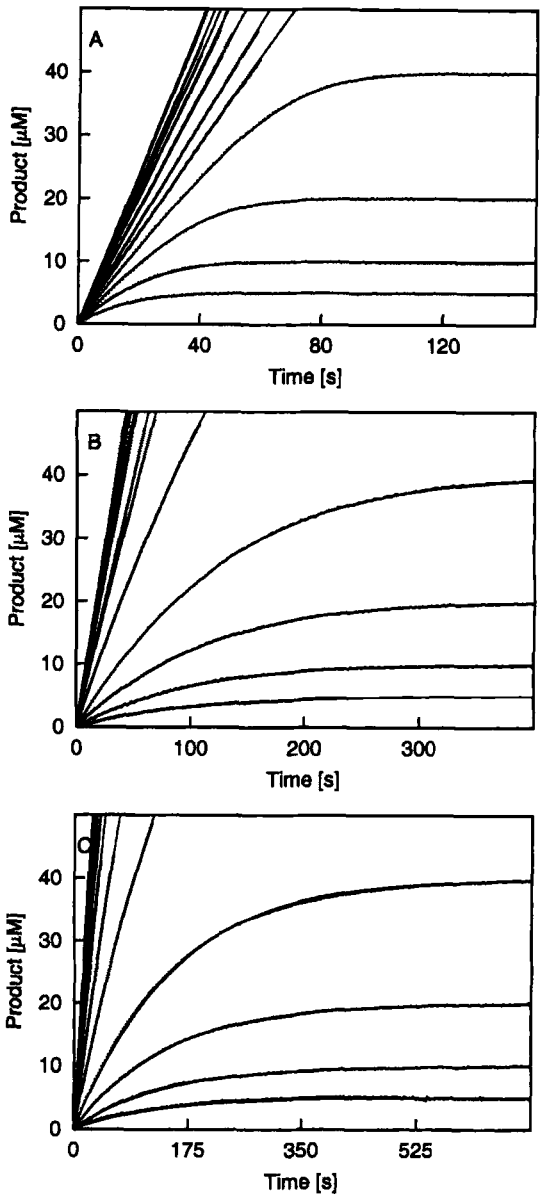

FIG. 4 Numerically solved solutions of differential equations fitted on entire progress curves: A, E107K; B, E107W; and C, E107Y.

could only be revealed by using progress curves analysis and a numerical integration method.

DISCUSSION

The empirical six parameter kinetic model (Scheme 1) seems to be valid for all cholinesterases.[2,5–7] The deviations from Michaelis–Menten pattern are expressed in factor a for inhibition and b for apparent activation.[6] It should be remembered that both parameters are less than unity.[2,5–7] The substrate concentrations around which one or the other deviation is detectable are given in the thermodynamic equilibrium constants K_1 and K_2. It should be emphasised that when one of the parameters a or b is approaching unity, then deviation described by this parameter can be omitted and, consequently, the appropriate equilibrium constant cannot be determined.[5] In contrast, more obviously visible deviation demands smaller ratios for a and b.

Theoretically, both initial rates as well as progress curve analysis should give the same kinetic constants describing inhibition and activation. It is easily seen from the results that this is not true in all cases. The reason is that the progress curves give a much higher reliability of the determined kinetic parameters.[16] Moreover, it is not a trivial task to estimate initial rates especially at very low substrate concentrations where initial portions of progress curves are nonlinear functions of time. The high precision of kinetic parameters is usually not required because of precision itself, but the goodness of fit can be a useful standard for discrimination between rival models.[17]

It is clear from the results that all kinetic parameters for the E107K mutant evaluated with different analysis methods do not differ significantly. It is a logical consequence because for this mutant both deviations, activation and inhibition, are easily seen even from the data obtained by initial rates measurements as shown in Fig. 1. This is also reflected in small factors for a and b. In contrast, it can be seen from Table I that the standard deviations of determined parameters by initial rate (section A) equations for E107W and E107Y are very similar to those for E107K, but activation was not considered. It is also obvious from Fig. 1 that the fitted curves for both enzymes missing activation agree very well with the initial rate data, but this is not the case when progress curves analysis is applied as displayed in Fig. 2. The latent substrate activation was determined in the next step where activation was considered, but only for E107W as seen in Table I under section C. The reason why the fitting was unsuccessful for the E107Y mutant is hidden due to the greater amount of enzyme used in this experiment. The consequence of higher enzyme concentration is reflected in greater omission of reaction time course data at low substrate concentration where non steady-state conditions occur.[15] We could avoid this problem by decreasing the enzyme concentration, but it would delay the experiment. It was decided rather to solve the problem by applying the numerical integrated method. The final results shown in Table I under section D indicate that both enzymes E107W and E107Y show latent substrate activation which could not be detected with initial rate analysis. The latency of activation is visible also in the values of factors a and b which are close to 1.

As mentioned before, all parameters evaluated by each individual analysis method do not differ significantly for E107K. The same is true for the other two mutants, but only in the case of constants k_3, K_2 and a. Acylation is the rate limiting step at low substrate concentration and, consequently, the second order kinetic constant k_i for the E107W and E107Y mutants differed more significantly when determined by different analysis methods. The parameter k_i has no effect on the rates at high substrate concentration because deacylation represented by k_3 becomes the slowest step during the substrate metabolism. It is obvious, therefore, that kinetic

parameters responsible for substrate activation k_i, K_1 and b cannot be determined sufficiently well or even that some of them can be lost by using classic initial rate analysis.

It has been found in recent studies[6,18] that an appropriate peripheral inhibitor or mutation at the rim of the gorge of AChE can mask apparent substrate activation. The exploration of this homotropic cooperative effect by *Drosophila* AChE using Triton X-100 and mutated enzymes[18] led to the hypothesis that E107 plays an important role in the initial binding of a substrate molecule on the free enzyme and, consequently, affects the entrance of another substrate molecule into the active site cleft. This could be a correct interpretation at first sight when only data obtained by initial rate measurements are taken into consideration. However, the detailed progress curves analysis in this work shows that all three tested mutants show high affinity (K_1) for the binding of the substrate to the free enzyme. Additionally, the values do not differ significantly from those for wild type enzyme.[5,6] These results could be in accordance with the assumption that the initial substrate binding site is located around D413[6] opposite to E107. It seems that mutation of glutamate 107 with a bulkier amino acid residue affects the acylation as seen from the decreased k_i, but reduces the modulation effect of the substrate molecule bound on the free enzyme (see factor b). The modulation is more obvious when a positive or negative charge is located at position 107 or, alternatively, when the entrance to the active site in the vicinity of E107 is more open[6] (W359L).

Finally, we could conclude with the following hypothesis. Insect acetylcholinesterases bind substrate with high affinity to free enzyme, but presumably the responsible initial contact site is not E107 in *Drosophila* AChE. The enhancement of steric blockades at the entrance of the gorge reduces the acylation rate constant, but obviously improves substrate orientation before it glides along the gorge to the catalytic triad. Additional charges at the rim of the gorge or enhanced entrance can disorientate substrate molecules which means in fact inhibition as seen from a decreased factor b, but demonstrated as apparent substrate activation.

Acknowledgements

The author thanks Dr Jure Stojan for his valuable comments on the manuscript and expresses gratitude to Dr Didier Fournier at Université Paul Sabatier, Toulouse, France for kindly supplying *Drosophila melanogaster* AChEs. This work was supported by the Ministry of Science and Technology of the Republic of Slovenia.

References

[1] Marcel, V., Palacois, L.G., Pertuy, C., Masson, P. and Fournier, D. (1998), *Biochem. J.* **329**, 329–334.
[2] Stojan, J., Golicnik, M., Estour, F., Froment, M.T. and Masson, P. *Biochem. J.*, (in press)
[3] Cauet, G., Friboulet, A. and Thomas, D. (1987), *Biochem. Cell. Biol.* **65**, 529–535.
[4] Szegletes, T., Mallender, W.D., Thomas, P.J. and Rosenberry, T.L. (1999), *Biochemistry* **38**, 122–133.
[5] Stojan, J., Marcel, V., Estrada-Mondaca, S., Klaébé, A. and Fournier, D. (1998), *FEBS Lett.* **440**, 85–88.
[6] Golicnik, M., Fournier, D. and Stojan, J. (2001), *Biochemistry* **40**, 1214–1219.
[7] Stojan, J., Marcel, V. and Fournier, D. (1999), *Chem.–Biol. Interact.* **119–120**, 137–146.
[8] Cha, S. (1968), *J. Biol. Chem.* **243**, 820–825.
[9] Bader, G. and Deuflhard, P. (1983), *Numer. Math.* **41**, 373–398.
[10] Stojan, J. (1997), *J. Chem. Inf. Comput. Sci.* **37**, 1025–1027.
[11] Fournier, D., Bride, J.M., Hoffman, F. and Karch, F. (1992), *J. Biol. Chem.* **267**, 14270–14274.
[12] Estrada-Mondaca, S. and Fournier, D. (1998), *Proteins Expression Purif.* **12**, 166–172.
[13] Ellman, G.L., Courtney, K.D., Andres, V. and Featherstone, R.M. (1961), *Biochem. Pharmacol.* **7**, 88–95.
[14] Duggleby, R.G. (1986), *Biochem. J.* **235**, 613–615.
[15] Laidler, K. and Bunting, J. (1973) *Enzyme Kinetics* (Calderon Press, Oxford).
[16] Marcus, M. and Plesser, T. (1981) *Kinetic Data Analysis* (Plenum Publishing Corporation, New York).
[17] Manervick, B. (1982), *Meth. Enzymol.* **87**, 370–390.
[18] Marcel, V., Estrada-Mondaca, S., Magné, F., Stojan, J., Klaébé, A. and Fournier, D. (2000), *J. Biol. Chem.* **275**, 11603–11609.

APPENDIX

Equation (3) can be transformed into a new implicit function F_e:

$$F_e = \left(1 - \frac{[P]_t}{[S_0]}\right)\left(1 - \frac{b[P]_t}{(K_1 + b[S_0])}\right)^{(1-b)/b} - e^{\beta} = 0$$

where

$$\beta = \frac{([P]_t - k_{+3}E_0 t)k_i}{k_3}$$

The derivative of F_e with respect to $[P]_t$ is

$$F'_e = -\frac{1}{[S_0]}\left(1 - \frac{b[P]_t}{(K_1 + b[S_0])}\right)^{(1-b)/b} - \left(1 - \frac{[P]_t}{[S_0]}\right)\frac{1-b}{(K_1 + b[S_0])} \times \left(1 - \frac{b[P]_t}{(K_1 + b[S_0])}\right)^{(1-2b)/b} - \frac{k_i}{k_3}e^{\beta}$$

and the solution of F_e is obtained iteratively using the ratio as a correction in each step as shown in the following equation:

$$[P]_t^{n+1} = [P]_t^n - \frac{F_e}{F'_e}$$

The process can be repeated until correction makes no appreciable difference to $[P]_t$.